Journal of Physiology (1992), **458**, *pp.* 41–67
With 16 *figures*
Printed in Great Britain

THREE POTASSIUM CHANNELS IN RAT POSTERIOR PITUITARY NERVE TERMINALS

BY KLAUS BIELEFELDT, JANET L. ROTTER AND MEYER B. JACKSON
From the Department of Physiology, University of Wisconsin Medical School, Madison, WI 53706, USA

(*Received 7 October 1991*)

SUMMARY

1. The patch clamp technique was used to investigate the K^+ channels in the membranes of nerve terminals in thin slices prepared from the rat posterior pituitary.

2. Depolarization of the membrane produced a high density of K^+ current. With a holding potential of −80 mV, test pulses to +50 mV activated a K^+ current which was inactivated by 65% within 200 ms. Hyperpolarizing prepulses enhanced the transient K^+ current, with half-maximal enhancement at −87 mV. Depolarizing prepulses reduced or eliminated the transient K^+ current.

3. In cell-attached patches formed with pipettes containing 130 mM KCl, three types of K^+ channel could be distinguished on the basis of single-channel properties. One channel had a conductance of 33 pS and was inactivated with a time constant of 18 ms. A second channel had a conductance of 134 pS and was inactivated with a time constant of 71 ms. A third channel had a conductance of 27 pS, was activated relatively slowly with a time constant of 65 ms, and was not inactivated during test pulses of up to one second in duration.

4. Inactivation of the whole-cell K^+ current was a biphasic process with two exponential components. The fast component had a time constant of 22 ms (at +50 mV), corresponding well with the time constant of decay of average current in cell-attached patches containing only the rapidly inactivating K^+ channel. The slow component of inactivation had a time constant of 104 ms (at +50 mV), which was similar to but slightly slower than the time constant of decay of the average current in cell-attached patches containing only the slowly inactivating K^+ channel. Inactivation of the slow transient K^+ current became more rapid with increasing depolarization.

5. The low-conductance rapidly inactivating K^+ channel had a lower voltage threshold for activation than the other two K^+ channels.

6. Both inactivating K^+ channels were enhanced in a similar manner by prior hyperpolarization. There was no difference with regard to voltage mid-point or steepness.

7. The large-conductance slowly inactivating K^+ channel was activated by Ca^{2+} at the inner membrane surface. The resting intracellular Ca^{2+} was sufficiently high to produce significant activation of this channel without depolarization-induced Ca^{2+} entry.

MS 9793

8. Removal of Ca^{2+} from the bathing solution produced a -10 mV shift in the voltage dependence of enhancement of both transient K^+ currents by prior hyperpolarization. This could be explained as a surface charge effect.

9. Tetraethylammonium blocked all three K^+ channels, but was most effective in blocking the rapidly inactivating low-conductance K^+ channel. Charybdotoxin did not reduce K^+ current in the preparation. Dendrotoxin selectively blocked the low-conductance, non-inactivating K^+ channel.

10. The low-conductance, rapidly inactivating K^+ channel has many properties that are similar to transient K^+ channels described in nerve cell bodies. The low-conductance non-inactivating K^+ channel does not resemble channels previously described in nerve cell bodies, including the hypothalamic cell bodies from which these nerve endings originate. This K^+ channel may be a specific axonal or nerve terminal membrane component.

11. The complex voltage, time and Ca^{2+} dependence of these K^+ channels is consistent with a function in the regulation of secretion from the posterior pituitary by frequency and pattern of electrical activity.

INTRODUCTION

Potassium channels can exert a powerful influence on the excitability of nerve endings. By controlling action potential repolarization and the threshold for action potential generation, K^+ channels can regulate the amount of transmitter secretion, and thus control synaptic efficacy (Benoit & Mambrini, 1970; Jan, Jan & Dennis, 1977; Kandel & Schwartz, 1982; Hochner, Klein, Schacher & Kandel, 1986; Augustine, 1990). Secretion from nerve endings can be altered by previous electrical activity and by chemical signals. By virtue of their complex voltage dependence and their coupling to receptors for many known intercellular signalling molecules, K^+ channels have the capacity to serve as transducers, both for signals that are chemical in nature and for signals that are encoded in the frequency or pattern of activity. Thus, investigating the properties of the K^+ channels in nerve endings can contribute much to our understanding of how secretion from nerve endings is controlled. Much is known about the K^+ channels in non-neuronal secretory cells (Marty, 1981; Wong, Lecar & Adler, 1982; Marty & Neher, 1984; Oxford & Wagoner, 1989). However, a comparable understanding of the K^+ channels in the membranes of nerve endings, particularly vertebrate nerve endings, is lacking.

The nerve endings of the posterior pituitary release the neuropeptides vasopressin and oxytocin. Secretion from the posterior pituitary is triggered by Ca^{2+} entry during presynaptic action potentials (Douglas & Poisner, 1963; Nordmann, 1983). This Ca^{2+}-dependent secretion is in turn modulated by stimulus frequency (Dreifuss, Kalnins, Kelly & Ruf, 1971; Gainer, 1978; Dutton & Dyball, 1979; Bondy, Gainer & Russell, 1987), complex patterns of activity (Dutton & Dyball, 1979; Shaw, Bicknell & Dyball, 1984; Bicknell, Brown, Chapman, Hancock & Leng, 1984; Cazalis, Dayanathi & Nordmann, 1985; Nordmann & Stuenkel, 1986), and peptides (Bondy, Whitnall, Brady & Gainer, 1989). These nerve endings are thus subject to many interesting forms of control and are an important site for regulation of neuroendocrine function.

The high density and large size of the nerve endings in the posterior pituitary make

this an excellent preparation for the study of neuronal secretion mechanisms. Optical techniques have probed the underlying conductance mechanisms of the posterior pituitary (Salzberg, Obaid, Senseman & Gainer, 1983; Salzberg & Obaid, 1988; Obaid, Flores & Salzberg, 1989) and have demonstrated the broadening of action potentials by high frequency stimulation (Gainer, Wolfe, Obaid & Salzberg, 1986). Electrophysiological studies in intact tissue revealed stimulus-activated channels (Mason & Dyball, 1986) and confirmed the existence of frequency-dependent broadening of the nerve terminal action potential (Bourque, 1990; Jackson, Konnerth & Augustine, 1991). Experiments in dissociated pituitary nerve endings have revealed additional interesting properties of neurosecretory membranes (Lemos & Nowycky, 1989; Lim, Nowycky & Bookman, 1990; Thorn, Wang & Lemos, 1991).

K^+ channels clearly play a role in secretion from the posterior pituitary. Blockade of K^+ channels enhances peptide release (Bondy *et al.* 1987; Hobbach, Hurth, Jost & Racké, 1988) and broadens action potentials (Bondy *et al.* 1987; Salzberg & Obaid, 1988; Jackson *et al.* 1991). Inactivation of K^+ current also broadens action potentials (Jackson *et al.* 1991), thus contributing to the facilitation of neuropeptide secretion. Voltage clamp studies have recently demonstrated the presence of a transient K^+ current in the membranes of posterior pituitary nerve endings (Thorn *et al.* 1991; Jackson *et al.* 1991). In the present study we have characterized the channels that are responsible for the macroscopic K^+ current. This has permitted us to decompose the macroscopic K^+ current into components that can be resolved on the basis of kinetic properties, voltage dependence, Ca^{2+} dependence and drug sensitivity. Our studies showed that the transient K^+ current of this preparation is produced by the activation of two distinct K^+ channels. In addition, we found a third K^+ channel with slow activation kinetics and little if any inactivation. Thus, there are at least three types of K^+ channels in the membranes of posterior pituitary nerve endings, which can contribute to action potential repolarization and to the regulation of secretion.

METHODS

Slices. The thin slice technique (Edwards, Konnerth, Sakmann & Takahashi, 1989) was adapted to the posterior pituitary, as described by Jackson *et al.* (1991). Male rats ranging in age from 6 weeks to 3 months were killed by decapitation following CO_2 narcosis. The neurointermediate lobe of the pituitary was removed and chilled for 1–3 min in carbogen (95% O_2, 5% CO_2)-saturated ice-cold bathing saline (125 mM NaCl, 2·5 or 4 mM KCl, 26 mM $NaHCO_3$, 1·25 mM NaH_2PO_4, 2 mM $CaCl_2$, 1 mM $MgCl_2$, 10 or 20 mM glucose). The tissue was glued to a plastic block, and then reimmersed in ice-cold bathing saline. Slices 70 to 80 μm thick were cut with a vibratome and were either used immediately for recordings, or were kept in carbogen-saturated saline for up to 2 h. Recordings were made at room temperature while perfusing with carbogen-saturated bathing saline. Spherical structures visualized with Nomarski optics at the surface of these slices were judged to be nerve terminals by criteria discussed previously (Jackson *et al.* 1991).

Whole-cell currents. Patch pipettes for tight-seal voltage clamping (Hamill, Marty, Neher, Sakmann & Sigworth, 1981) were filled with 140 mM KCl, 10 mM EGTA, 4 mM ATP and 4 mM $MgCl_2$, buffered at pH 7·3 with 10 mM HEPES. An EPC-7 or EPC-9 patch clamp amplifier (Instrutech, Elmont, New York) was interfaced to an Atari computer for pulse application and data recording. Recordings were only used when the uncompensated series resistance was less than 12 MΩ. In most whole-cell recordings the uncompensated series resistance was close to 5 MΩ. Series resistance compensation was routinely used to reduce the effective series resistance by 50–70%. Leak currents were subtracted, where indicated in the results, by using the P/4 technique from a holding potential of −110 or −120 mV. For voltage jumps from −80 to +50 mV, the average

steady-state leak current was 0·13 nA. This was very small compared to the K^+ currents activated by such voltages. Thus the P/4 correction was small.

The capacitance and series resistance were determined by using the transient cancellation circuitry of the patch clamp amplifier (Marty & Neher, 1983). Theoretical analysis of the charging transients produced by a spherical structure with a cylindrical process such as an axon indicated that transient cancellation provides a valid measure of the capacitance of the nerve ending (Jackson, 1992). Cable analysis with small voltage steps indicated that the axon charging currents varied in time course, but were usually brief and relatively small (Jackson, 1992*a*, *b*). In the recordings used in this study, the settling time of the nerve terminal charging current was always less than 100 μs. The nerve terminals themselves are charged rapidly enough to study the kinetics of K^+ currents described here, but cable analysis alone cannot provide assurance that some of the observed K^+ current does not arise from poorly space-clamped axons. The best evidence that K^+ currents are well voltage clamped comes from comparisons with the results of single-channel experiments.

Single-channel currents. Single-channel currents were recorded in the cell-attached configuration with an EPC-9 patch clamp amplifier and with patch pipettes filled with 130 mM KCl, 2 mM $CaCl_2$, 1 mM $MgCl_2$, 10 mM HEPES, pH 7·3. Single-channel currents were recorded in excised inside-out patches, which were prepared by pulling the patch electrode away after changing the bathing solution to 150 mM KCl, 1 mM EGTA, 10 mM HEPES, pH 7·3.

Data analysis. Analysis of macroscopic and single-channel current was performed with the program REVIEW from Instrutech. This program was also used to fit data to sums of exponentials. Fits to the Boltzmann equation were performed with the program COSTAT (CoHort Software, Berkeley, CA, USA). Unless otherwise noted, we present arithmetic means ± standard error of mean.

RESULTS

Macroscopic K^+ current

Depolarizing pulses under voltage clamp from a holding potential of −80 mV to a test potential of +50 mV activated outward current that declined as the test potential was held constant (Fig 1*A*). The outward current was judged to be K^+ current by the following criteria. (1) The K^+ channel blockers tetraethylammonium (TEA) and dendrotoxin reduced the outward current (see *Pharmacology* below). (2) The tail current reversed near the computed K^+ Nernst potential with both 2·5 and 4 mM extracellular K^+. (3) Outward current with the same basic qualitative features was observed when intracellular Cl^- was replaced by gluconate, indicating that these were not Cl^- currents. The decline in outward current that occurred during the test pulse was judged to be inactivation of K^+ current by the following criteria. (1) Small secondary test pulses of 5 mV and 5 ms applied at various times during the main test pulse to +50 mV indicated that there was a conductance decrease concomitant with and proportional to the decline in current. (2) The reversal potential of the tail currents was the same (near the K^+ Nernst potential) for both brief 10 ms and long 200 ms test pulses. Furthermore, the interpretation of the outward current as a transient K^+ current was supported by all of the single-channel studies described below; the single-channel data were consistent with the basic voltage dependence and kinetics of the macroscopic current.

An inward current was seen during the first 1 or 2 ms of a test pulse, provided that there was no tetrodotoxin added to the bathing solution (Fig. 1*A*). This inward current extrapolated to zero near the Na^+ Nernst potential. In many experiments 1 μM tetrodotoxin was added to block this Na^+ current. Because the Na^+ current was inactivated so rapidly, omission of tetrodotoxin did not interfere with studies of the K^+ current after the first few milliseconds.

Based on the magnitude of Ca^{2+} current in the membranes of pituitary nerve terminals (Lemos & Nowycky, 1989), we expect Ca^{2+} current to be very small compared to the K^+ currents we have seen. A small increase in outward current following the addition of 100 or 200 μM cadmium (see *Divalent cation effects* below)

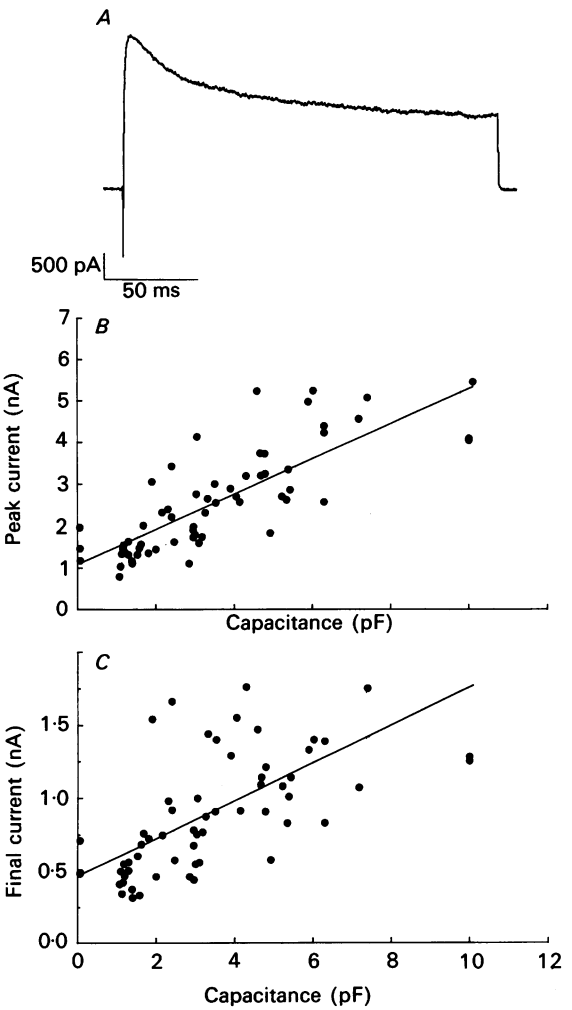

Fig. 1. Macroscopic K^+ current in nerve terminals. *A*, a voltage step from −80 to +50 mV activated K^+ current, which was inactivated by sustained depolarization. A small brief tetrodotoxin-sensitive inward Na^+ current can be seen at the beginning of the depolarizing test pulse. The nerve ending from which this recording was made had a capacitance of 3·9 pF. Whole-cell currents were recorded in this way from sixty-three nerve endings. In each recording peak current and final current (after 200 ms) were measured and plotted *versus* capacitance (*B* and *C*, respectively), with each recording contributing one point to each plot. The best-fitting lines are shown in each case. For peak K^+ current the slope was 0·442 nA pF^{-1}, the intercept was 1·11 nA, and the linear correlation coefficient was 0·80. For the final K^+ current the slope was 0·132 nA pF^{-1}, the intercept was 0·49 nA, and the linear correlation coefficient was 0·62. For both linear correlation coefficients, $P < 0·001$. P/4 leak correction was used on all of the measurements that provided data for this figure.

may be due to block of Ca^{2+} current. The evidence provided above for the identification of the outward current as K^+ current is also evidence that a concurrent inward Ca^{2+} current is relatively small.

To estimate the density of K^+ current, we plotted current *versus* capacitance (Fig. 1*B* and *C*). Peak and final K^+ current were taken from recordings such as shown in

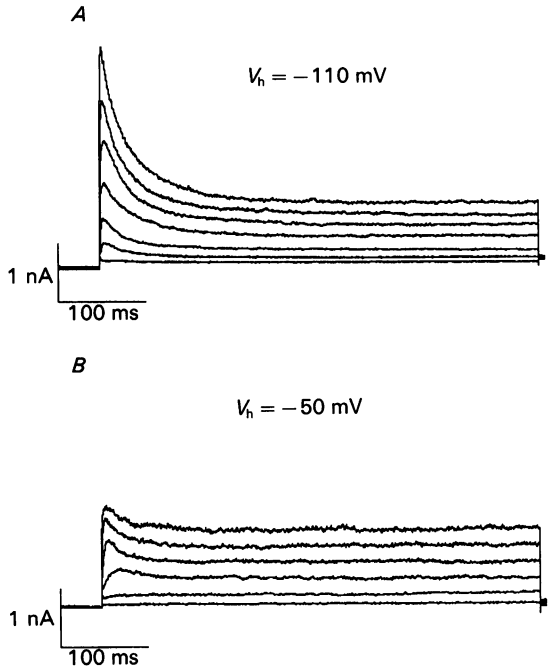

Fig. 2. K^+ currents were activated with different depolarizing test pulses following 1 s prepulses (V_h) to −110 mV (*A*) and −50 mV (*B*). Test pulses of 500 ms ranged from −60 to +60 mV in *A* and from −40 to +60 mV in (*B*). This membrane potential was held at −80 mV between pulses, which were applied at 8 s intervals. These experiments were done with P/4 leak correction.

Fig. 1*A*, from sixty-three different nerve endings. In all of these recordings the current was activated by voltage jumps from −80 to +50 mV. There was a strong correlation between K^+ current and membrane area (Fig. 1*B* and *C*), as estimated from membrane capacitance. The best-fitting lines from these plots were $1{\cdot}11+0{\cdot}42$ and $0{\cdot}49+0{\cdot}13C$ nA (C = nerve ending capacitance in pF) for the peak current and the current at 200 ms, respectively. The mean peak current density was $1{\cdot}8\pm0{\cdot}6$ mA cm^2 (mean ± S.D.; assuming a specific membrane capacitance of 1 μF cm^{-2}). Peak current was inactivated by an average of 65 ± 16% (mean ± S.D.) at 200 ms for the sixty-three recordings used to make Fig. 1*B* and *C*, and there was no significant correlation between the percentage of inactivation and nerve terminal capacitance. Thus, the nerve endings of the posterior pituitary have characteristic and reproducible components of transient and enduring K^+ current. The densities of these K^+ currents are high and thus are capable of exerting a strong influence on the excitability of these membranes.

Voltage dependence of macroscopic K^+ current

The K^+ current induced by a depolarizing step was a function of both test potential and holding potential (Fig. 2*A* and *B*). The threshold for activation was approximately −40 mV. With a holding potential of −110 mV the K^+ current was

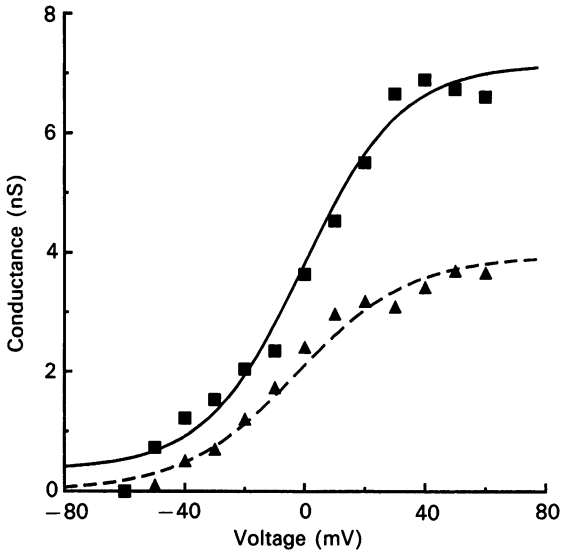

Fig. 3. Conductance *versus* voltage for transient (■) and non-inactivating (▲) K^+ current. The pulse protocol was as for Fig. 2*A*. The conductance was computed by dividing the current by the driving force ($V-E_K$), with E_K computed from the solution compositions. The current at the end of the 500 ms test pulse was taken as the non-inactivating current. This final current was subtracted from the peak current to obtain the transient current. The smooth curves are best fitting Boltzmann equations of the form:

$$G = G_{min} + \frac{G_{max} - G_{min}}{1 + e^{Z(V_m - V)}}$$

All four parameters, G_{min}, G_{max}, Z and V_m were varied to achieve the best fit. G_{min} and G_{max} are the conductance asymptotes at negative and positive voltages respectively, Z is the steepness factor and V_m is the mid-point for voltage dependence. Best-fitting values for Z were 0·061 and 0·053 for the transient and non-inactivating conductance, respectively. Best fitting values for V_m were −1 and −3 mV.

much larger than when the holding potential was −50 mV. When K^+ current was activated by jumping from a holding potential of −110 mV to a test potential of +50 mV, it inactivated by approximately 75%. In contrast, when the holding potential was −50 mV, the K^+ current was small and we saw very little inactivation. The conductance was computed by dividing current by the test voltage minus the computed K^+ Nernst potential ($V-E_K$; $E_K = -89$ mV), and plotted *versus* test voltage for both the transient and enduring components of K^+ current. These plots showed that conductance increased with test voltage and saturated above +30 mV (Fig. 3*A* and *B*). In nine experiments, the plots of conductance *versus* voltage consistently showed that between −40 and −20 mV some of the transient current was slightly higher than the best-fitting Boltzmann function (Fig. 3). This small

deviation from the theoretical curve is actually due to the presence of a low-threshold K^+ channel. Data presented below support the decomposition of transient K^+ current into separate components with different activation thresholds.

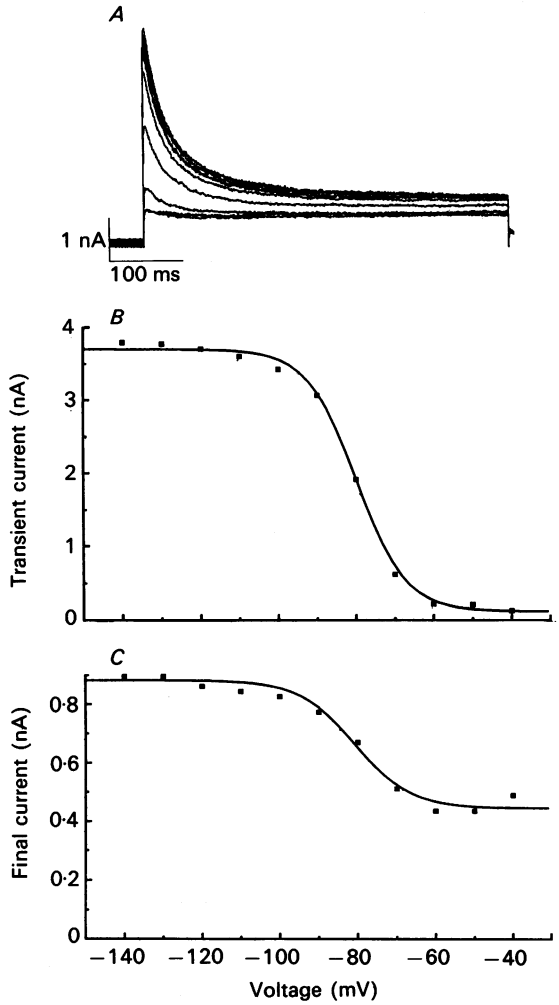

Fig. 4. K^+ current was enhanced by hyperpolarizing prepulses. *A*, currents activated by 500 ms test pulses to +50 mV are shown for a sequence of 1 s prepulses between −40 to −140 mV. Final current was taken as the current at the end of the test pulse. Transient current was taken as the peak minus the final current. Both transient and final current were enhanced by prior hyperpolarization. *B*, the transient K^+ current was plotted *versus* the prepulse potential and fitted to the Boltzmann equation (see legend of Fig. 3). The best fitting parameters were $V_m = -80$ mV and $Z = -0{\cdot}16$. *C*, the final current was plotted *versus* prepulse potential and fitted to a Boltzmann equation to give $V_m = -81$ mV and $Z = -0{\cdot}14$. Mean values are given in the text. Leak subtraction was not necessary since pulses to the same test potential produce the same amount of leak current.

The effect of holding potential is illustrated more clearly in Fig. 4*A*, where responses to the same test potentials are shown following 1 s prepulses to increasingly hyperpolarized potentials. Figure 4*B* and *C* shows that the voltage dependence of

this enhancement process is steeper than for the activation of the K^+ current by depolarization (Fig. 3). This effect of hyperpolarization has also been shown for K^+ currents in isolated nerve endings (Thorn *et al.* 1991), and is characteristic of a variety of transient outward currents described in many different preparations (Hagiwara, Kusano & Saito, 1961; Neher, 1971; Connor & Stevens, 1971; Rogawski, 1985; Cobbett, Legendre & Mason, 1989; Zagotta & Aldrich, 1990). Boltzmann functions fitted the curves of Fig. 4*B* and *C* very well. In seven such experiments the average mid-point voltages were -87 ± 2 mV for the transient current (peak current minus final current) and -82 ± 2 mV for the enduring current. The steepness of these plots was used to estimate the number of gating charges that would have to cross the membrane completely to generate the observed voltage dependence. These gating charge numbers were $2{\cdot}9 \pm 0{\cdot}3$ for the transient current and $4{\cdot}0 \pm 0{\cdot}6$ for the enduring current. A Student's *t* test shows that the probabilities that these means are produced by sampling from the same population is between 0·05 and 0·10. Thus, the significance of these small differences is not clearly established by statistical criteria.

Channel properties

The high density of macroscopic K^+ current suggested that a high proportion of patches should contain K^+ channels. This was confirmed in single-channel recordings from cell-attached patches, with patch pipettes filled with 130 mM KCl to enhance current through K^+ channels. In 89% of the patches ($n = 75$), single-channel currents appeared (Fig. 5) during depolarizing voltage steps comparable to the voltage steps used to activate macroscopic K^+ currents in whole-cell experiments. These single-channel currents were judged to be K^+ currents by the following criteria. (1) Replacement of K^+ with *N*-methylglucamine in the patch pipette resulted in recordings in which no inward single-channel currents were observed ($n = 10$). (2) The channel currents reversed near a membrane potential of zero under conditions in which the K^+ concentration was nominally symmetrical (we have not determined the intracellular K^+ concentration, but we assumed it is similar to that of our cell-attached pipette solutions, and we used the average resting potential of -60 mV. (3) The kinetics and voltage dependence of the different K^+ channel types corresponded well with the different components of macroscopic K^+ current.

K^+ channels with different properties were seen in different patches. We saw channels with either high or low conductances. The low-conductance channels could be further subdivided into two types based on kinetic properties and voltage dependence (see Figs 7 and 8 below). Thus, there are at least three kinds of K^+ channels in neurohypophysial membranes. These three K^+ channel types all had roughly linear single-channel current–voltage plots, which reversed near -60 mV pipette potential (0 mV membrane potential) in nominally symmetrical K^+ (Fig. 6). Although the channels required strong depolarization to be activated, single-channel currents could be recorded over a wide range of voltage by examining the channel currents that appeared on the tail of a depolarizing test pulse (Fig. 5). In 130 mM K^+, the single-channel conductances were 33 ± 2 pS ($n = 15$), 134 ± 18 pS ($n = 8$), and 27 ± 3 pS ($n = 8$) for the low-conductance rapidly inactivating channel, the high-conductance slowly inactivating channel, and the low-conductance non-inactivating channel, respectively.

To illustrate the different kinds of kinetic behaviour, many single-channel records from a given patch were averaged (Fig. 7). These recordings were made from patches having only one type of channel. The averages showed that one of the low-conductance K^+ channels was activated rapidly and inactivated with a time constant

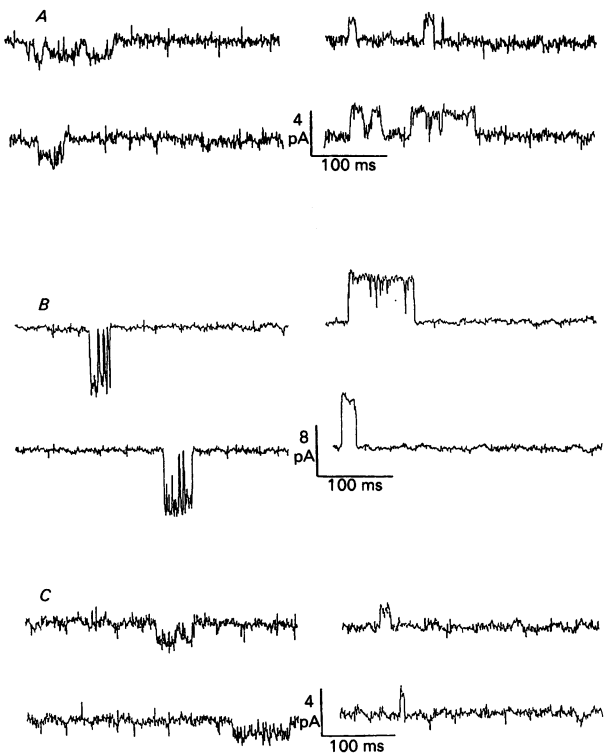

Fig. 5. Single K^+ channel currents in cell-attached patches. The traces on the left side of each part of the figure were activated by 300 ms depolarizing pulses from a membrane potential of -110 to $+50$ mV (membrane potential was estimated for pipette command potential changes from $+50$ to -110 mV, assuming a terminal resting potential of -60 mV). These pulses were similar to those used in whole-cell experiments to produce the macroscopic current responses in Fig. 2*A*. The traces on the right side were recorded on the tail of the depolarizing pulses. For these single-channel tail currents the pipette potential was 0 mV, corresponding to a membrane potential of -60 mV. Three types of channels were observed. These were a low-conductance rapidly inactivating channel (*A*), a high-conductance slowly inactivating channel (*B*), and a low-conductance slowly activating channel (*C*). The kinetic behaviour of these channels is illustrated in Fig. 7.

of $17{\cdot}6 \pm 1{\cdot}1$ ms ($n = 12$; Fig. 7*A*). In some patches with the other low-conductance K^+ channel, the average current was activated slowly with a time constant of 65 ± 15 ms ($n = 7$). This channel was not inactivated significantly during 300 ms test pulses (Fig. 7*C*). The high-conductance K^+ channel exhibited kinetic behaviour that was distinct from the two low-conductance K^+ channels. Averages of current from patches with the high-conductance K^+ channel inactivated with a time constant of 71 ± 15 ms ($n = 4$; Fig. 7*B*).

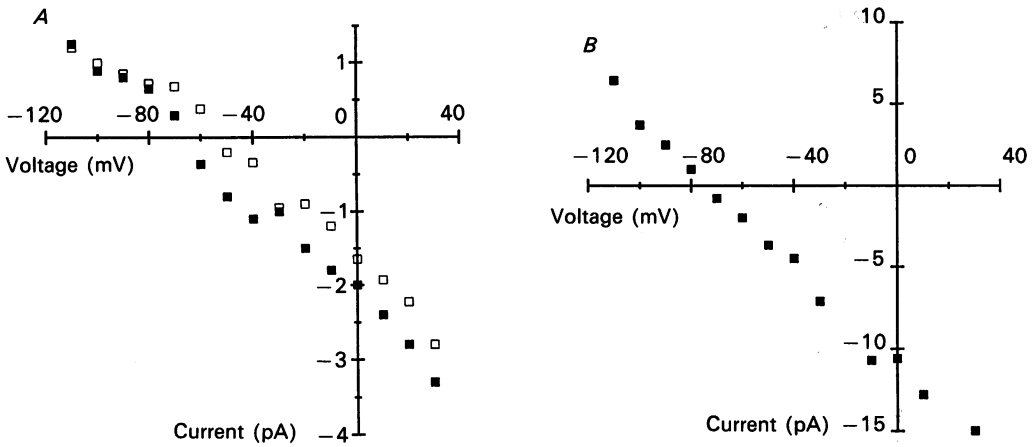

Fig. 6. Single-channel current–voltage plots. Single-channel currents from patches containing each of the three channel types were plotted *versus* membrane potential. Single-channel currents were recorded either with depolarizing pulses (Fig. 5, left) or on the tails of depolarizing pulses (Fig. 5, right). The best-fitting lines were used to estimate conductance and reversal potential. In *A*, ■ represents the low-conductance rapidly inactivating channel (Fig. 5*A*), which had a conductance of 33 ± 2 pS ($n = 15$); □ represents the low-conductance slowly activating channel (Fig. 5*C*), which had a conductance of 27 ± 3 pS ($n = 8$). In *B* current is plotted for the high-conductance slowly inactivating channel, which had a conductance of 134 ± 18 pS ($n = 8$).

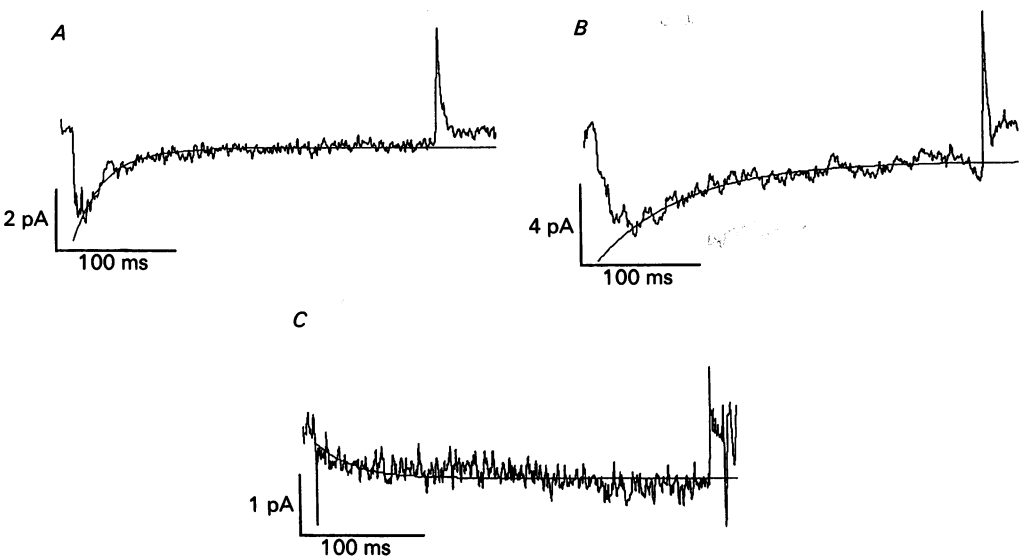

Fig. 7. Averages of fifty single-channel records produced by 300 ms voltage pulses from −110 to +50 mV. *A*, an average of fifty single-channel records from a patch with a low-conductance rapidly inactivating channel (Fig. 5*A*). The decay of average current was fitted by a single exponential with a time constant of 25 ms. *B*, an average of fifty single-channel records from a patch with a high-conductance slowly inactivating channel (Fig. 5*B*). The best-fitting exponential had a time constant of 67 ms. *C*, an average of fifty single-channel records from a patch with a low-conductance non-inactivating channel (Fig. 5*C*). The best-fitting exponential had a time constant of 27 ms. Average time constants for inactivation in cell-attached patches are presented in the text.

Not only were these channels different in terms of conductance and kinetic properties, but pulses to different test potentials in cell-attached patches showed that the different K^+ channel types had different voltage thresholds. Figure 8 shows averages of fifty sweeps, recorded from patches with only one kind of K^+ channel. In

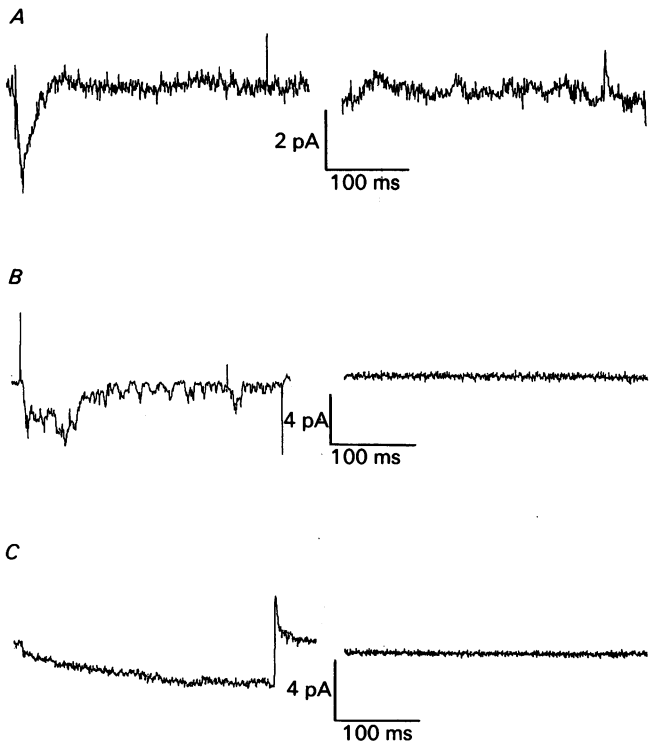

Fig. 8. Differences in thresholds of the K^+ channels. In patches with only one channel type, the averages of fifty sweeps were compared for pulses to membrane potentials of +30 and −30 mV. In *A* the low-conductance rapidly inactivating channel was activated at both voltages. In *B* the high-conductance slowly inactivating channel was activated at +30 mV, but not a single channel opening was observed in fifty sweeps at −30 mV. In *C* the low-conductance non-inactivating channel behaved similarly to the high-conductance channel in *B*; there were no channel openings at −30 mV.

patches containing the high-conductance channel or the low-conductance non-inactivating channel, single-channel openings were never seen with pulses to membrane potentials of −30 mV (pipette potential of +30 mV). The average was consequently completely flat (Fig. 8*B* and *C*). Channels were clearly present in these patches, as demonstrated by the high activity when voltage was pulsed to +30 mV. Patches with the low-conductance rapidly inactivating channel behaved differently. In patches containing these channels, test pulses to −30 mV generated positive channel currents, albeit at a lower frequency than with test pulses to +30 mV (Fig. 8*A*). This difference in threshold of activation of the two transient channels is supported by data presented below on the kinetics of activation (Fig. 9).

In the interest of simplifying the ensuing discussion, we will use the term A_f to denote the channel that produces the rapidly inactivating transient current. Because data presented below indicates that the slowly inactivating transient current is Ca^{2+}-activated, we will denote it as K^+_{Ca}. The non-inactivating K^+ channel will be referred to as the D channel. In 45% of the patches with K^+ channels (34 of 75) the A_f channel was the only K^+ channel seen. Another 15% of the patches had only K^+_{Ca} channels.

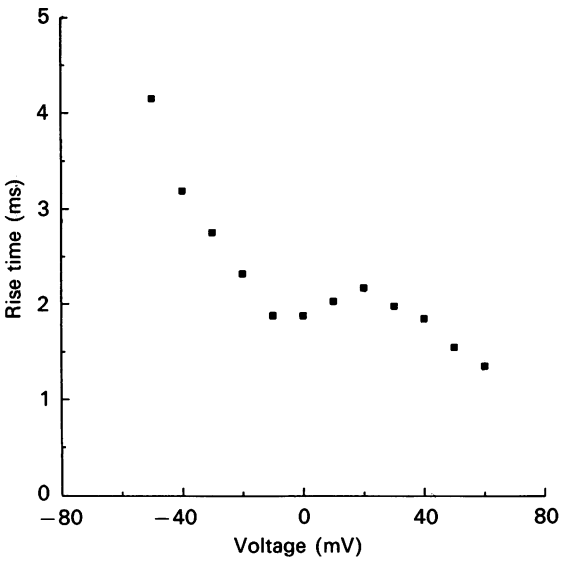

Fig. 9. K^+ current rise time *versus* voltage. The time to reach 90% of peak was measured for whole-cell currents similar to those in Fig. 2*A*, evoked by depolarizations from −110 mV to various test potentials. Tetrodotoxin was added so that Na^+ current did not obscure the rapid activation of K^+ current. P/4 leakage correction was employed.

In 16% of the patches only the D channel was found. The remaining 24% of the patches with channels contained two or more K^+ channel types. The frequency with which patches with these different channel types were encountered is consistent with the proportion of different components of K^+ current in whole-cell recordings. The incidence of patches with mixtures of channel types is consistent with a random distribution of channels on the surface of the nerve terminal membrane. Thus, it is unlikely that the different K^+ channels are segregated into different domains of membrane. All three channel types were also seen in cell attached patches using solutions containing 10 mM EGTA. Thus, preventing Ca^{2+} entry through the patch did not eliminate the activity of any of these channels.

Kinetics of activation and inactivation of macroscopic K^+ currents

With test pulses to +60 mV K^+ currents reached 90% of maximum in 1·5 ms. At less positive voltages, activation was slower. Plots of rise time (time to reach 90% of peak current) *versus* voltage revealed two phases to the voltage dependence of activation rate (Fig. 9). This behaviour was observed in nine such experiments.

Currents activated by the smallest voltage steps required 6–7 ms to reach 90% of peak, and this time grew shorter as the test pulses became more positive, reaching a local minimum of approximately 2 ms at −10 mV, after which the activation time became longer, peaked at +20 mV, and then went down again. This voltage dependence of activation time provides additional evidence for the decomposition of K^+ current into different components through different K^+ channels. Both transient K^+ channels were activated rapidly by strong depolarizations, but different voltage

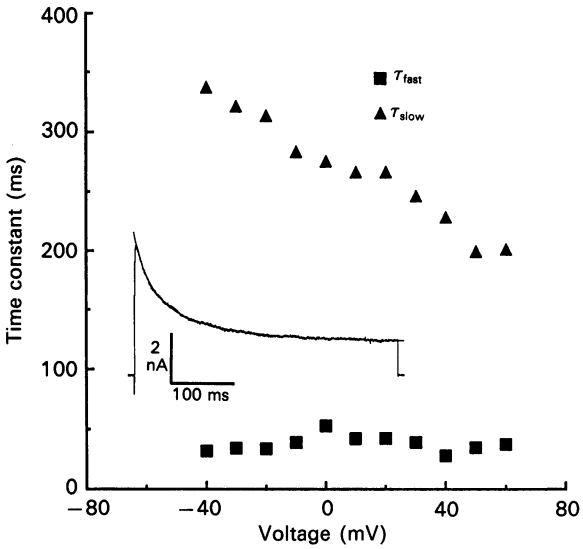

Fig. 10. Biphasic inactivation kinetics of whole-cell K^+ currents. The inset shows the best fitting sum of two exponentials drawn through a recording of K^+ current activated by a depolarizing 500 ms pulse from −80 to +50 mV. The fast component had a time constant of 19 ms and an amplitude of 1·43 nA. The slow component had a time constant of 79 ms and an amplitude of 1·66 nA. Average values are given in the text. Time constants were measured for currents activated by pulses from −110 mV to various test potentials, and plotted *versus* the voltage of the test potential.

thresholds would explain the biphasic voltage dependence of rise time in Fig. 9. The early decrease in rise time represents the activation of the A_f channel, which has a lower threshold (Fig. 8). When the higher threshold of the K^+_{Ca} channel was reached (*ca.* 0 mV), its activation was at first slow, so it prolonged the rise time. This produced the local maximum of Fig. 9. With stronger depolarizations, the activation of the higher threshold channel became more rapid. Both of the transient K^+ channels are activated rapidly enough to repolarize action potentials.

Inactivation of macroscopic K^+ current also exhibited distinct kinetic phases. The time course of inactivation was well described by a sum of two exponentials (Fig. 10, inset). The mean values of the time constants of inactivation for pulses from −80 to +50 mV were 21·6 ± 0·9 ms and 104 ± 5 ms (n = 63). Test pulses as long as 1 s showed a flat steady-state K^+ current with no further inactivation detectable. Plots of the two time constants of inactivation *versus* voltage revealed that the slow component

of inactivation was accelerated by higher test potentials (Fig. 10). The slight increase in the time constant of the fast component of inactivation was not significant.

We also examined the kinetics of inactivation as a function of the voltage of the prepulse. The time constants of inactivation were independent of prepulse potential

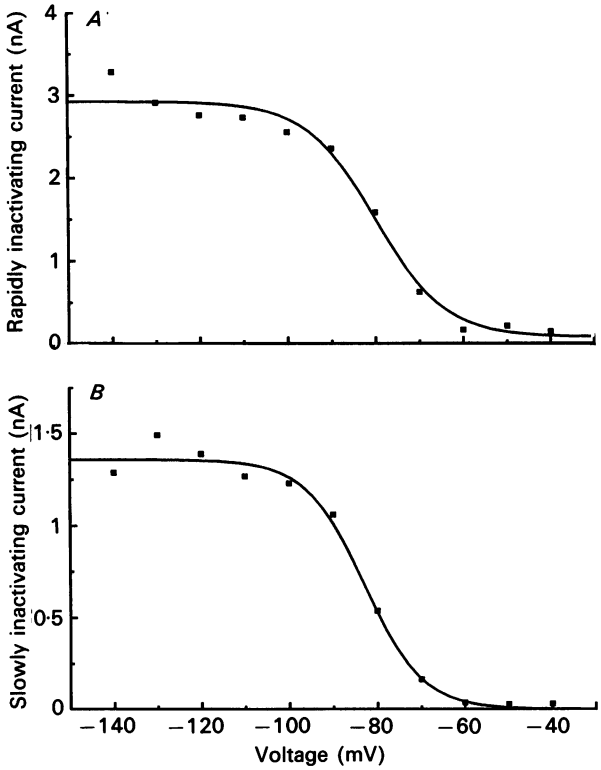

Fig. 11. Amplitudes of rapidly (*A*) and slowly (*B*) inactivating components of whole-cell K^+ current *versus* prepulse potential. Currents were evoked by 500 ms test pulses to +50 mV following 1 s prepulses to various potentials from −40 to −140 mV (as in Fig. 4*A*). The decaying phases of these currents were fitted to a sum of two exponentials, as in Fig. 10. The amplitudes of the two components were then plotted *versus* prepulse potential. These plots were fitted to a Boltzmann equation (see legend of Fig. 3). Averages of the best-fitting parameters are given in the text.

between −40 and −140 mV (data not shown). Both the rapidly and slowly inactivating components of K^+ current were strongly enhanced by hyperpolarizing prepulses (Fig. 11). This effect mirrored the enhancement of the total transient current (Fig. 4). As was found with the transient and enduring currents (Fig. 4), the plots of the rapidly and slowly inactivating components were well fitted by a Boltzmann equation (Fig. 11). The average voltage mid-points from six experiments were -86 ± 2 and -90 ± 4 for the rapid and slow components, respectively. The average gating charges were $2{\cdot}6\pm0{\cdot}2$ and $2{\cdot}8\pm1{\cdot}2$, respectively. Thus, the two transient K^+ channels were not distinguishable in terms of the voltage dependence of enhancement by a hyperpolarizing prepulse.

Divalent cation effects

Previous studies have suggested that many nerve terminal membranes contain Ca^{2+}-activated K^+ channels (Augustine & Eckert, 1982; Bartschat & Blaustein, 1984; Mallart, 1985; Lemos, Nordmann, Cooke & Stuenkel, 1986; Obaid *et al.* 1989;

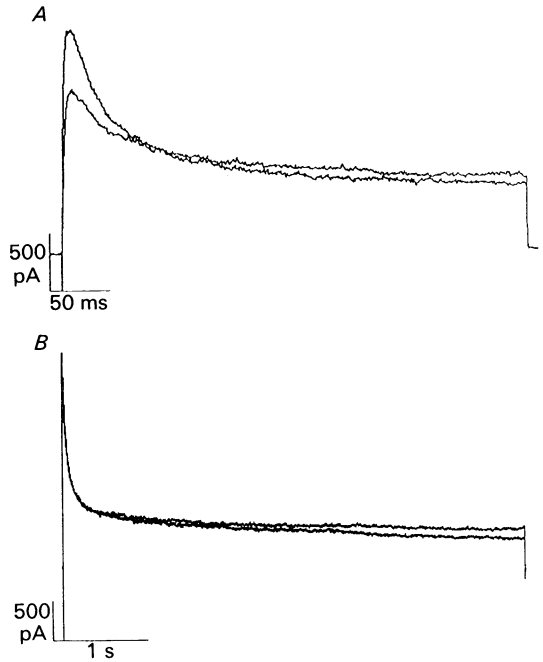

Fig. 12. The effect of Ca^{2+} removal and of 100 μM cadmium on K^+ current. *A*, pulses (400 ms) from −80 to +10 mV activated K^+ current. After replacing the control bathing medium (containing 2 mM Ca^{2+}; see Methods) with a solution of the same composition except with 0 Ca^{2+}, the K^+ current activated by a voltage step of the same size was reduced. *B*, addition of 100 μM cadmium (added as $CdCl_2$) without removing Ca^{2+} produced a slight increase in the K^+ current at the beginning of the 5 s voltage step from −100 to +10 mV, but the K^+ current was reduced later in the pulse.

Lindgren & Moore, 1989; Obaid & Salzberg, 1991). We first tested the effect of eliminating Ca^{2+} entry on whole-cell K^+ current (Fig. 12). Removal of Ca^{2+} from the bathing solution and addition of 100 μM cadmium had different effects. Cadmium (four experiments with 100 μM and three experiments with 200 μM) produced a slight increase (10–15%) in the K^+ current at the peak and early in the test pulse, probably due to block of the small inward Ca^{2+} current. But late in the pulse cadmium reduced the K^+ current (Fig. 12*B*). In contrast, calcium removal reduced peak outward current (Fig. 12*A*). A shorter pulse is shown with Ca^{2+} removal to demonstrate this effect clearly. With a longer depolarization in Ca^{2+}-free bathing solution, a late reduction of K^+ current appeared (data not shown), which was similar to that resulting from cadmium addition (Fig. 12*B*). The currents shown in Fig. 12 were

evoked by voltage steps to +10 mV, and with 0·5 mM EGTA in the patch pipette rather than 10 mM EGTA. These conditions have previously been shown to allow increases in $[Ca^{2+}]_i$ of a few hundred nanomolar (Jackson *et al.* 1991). Furthermore, 100 μM cadmium blocks Ca^{2+} spikes and stimulus-induced capacitance changes in this preparation (data not shown), indicating its effectiveness in blockade of Ca^{2+} current.

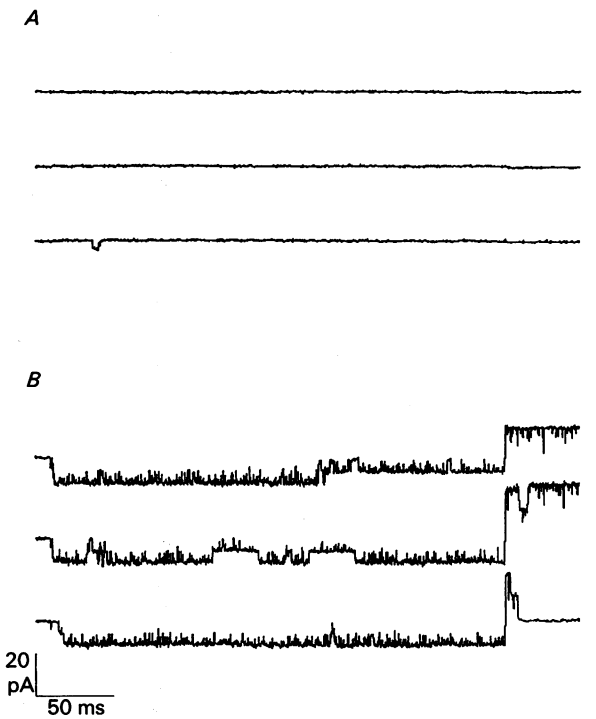

Fig. 13. K^+_{Ca} channel currents in excised patches. Initial recordings in the cell-attached mode showed that the patch contained the K^+_{Ca} channel and produced recordings similar to those shown in Fig. 5*B*. Before excision the bathing solution was changed to one with 1 mM EGTA and no added Ca^{2+}. Excision into this solution virtually abolished channel activity (*A*). The bathing solution was then changed to one with 1 mM EGTA and 941 μM Ca^{2+} (1 μM free Ca^{2+}; computation according to Carl & Sanders, 1989), resulting in channel activity much higher than was ever seen in the cell-attached configuration (*B*). Scale bars in *B* also apply to *A*.

The reduction in late K^+ current produced both by Ca^{2+} removal and by cadmium addition suggested the presence of a Ca^{2+}-activated K^+ channel. Experiments with excised inside-out patches showed that Ca^{2+} at the inner membrane surface activated the K^+_{Ca} channel (Fig. 13). In patches for which on-cell recordings revealed the K^+_{Ca} channel, excision into a solution with EGTA and no added Ca^{2+} blocked activity almost completely (Fig. 13*A*). Subsequently, increasing the free Ca^{2+} to 1 μM dramatically increased the activity of this channel in six experiments (Fig. 13*B*). Ca^{2+} at the inner membrane surface did not influence the other two K^+ channels.

A reduction in peak whole-cell K^+ current was seen when Ca^{2+} was removed from the bathing solution but not when cadmium was added (Fig. 12). The apparent contradiction between the two results shown in Fig. 12*A* and Fig. 12*B* can be reconciled by examining the effect of Ca^{2+} removal on K^+ current following

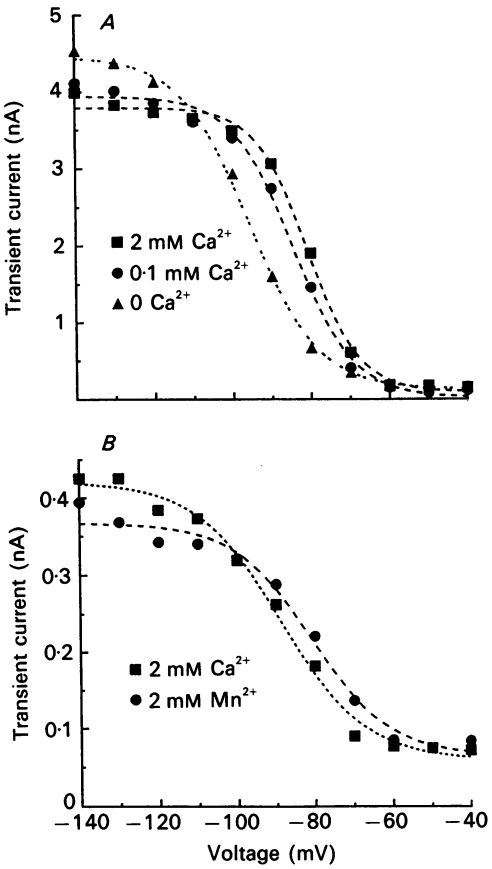

Fig. 14. Plots of transient K^+ current *versus* potential of a hyperpolarizing prepulse. As in Fig. 4, prepulses of 1 s duration were varied between −40 and −140 mV. The K^+ current was then activated by 500 ms pulses to +50 mV. The current at the end of these pulses was subtracted from the peak current to give the transient current. Best-fitting Boltzmann functions were drawn for each experiment (see legend of Fig. 3). *A*, removal of Ca^{2+} shifted the curve 14 mV to the left. Reduction of the Ca^{2+} to 0·1 mM shifted the curve 5 mV to the left. *B*, replacement of 2 mM Ca^{2+} with 2 mM manganese shifted the curve 8 mV to the right.

hyperpolarizing prepulses. A sequence of pulses similar to that shown in Fig. 4, with prepulses varying between −40 and −140 mV, showed that the reduction of K^+ current by Ca^{2+} removal can be overcome by hyperpolarizing prepulses (Fig. 14*A*). This figure shows that Ca^{2+} removal shifts the voltage dependence in the negative direction; $\Delta V_m = -10 \pm 2$ mV ($n = 3$; see Fig. 3 for definition of V_m). When the rapidly and slowly inactivating components of K^+ current were determined by curve fitting and examined separately, they both were reduced by Ca^{2+} removal and

showed similar enhancement by hyperpolarizing prepulses (data not shown). Reducing Ca^{2+} in the bathing solution to 0·2 mM had no discernable effect, but at 0·1 mM Ca^{2+} a small negative shift was evident (Fig. 14*A*). Replacement of 2 mM Ca^{2+} by 2 mM manganese shifted the voltage dependence in the positive direction (Fig. 14*B*), indicating that manganese was more effective than Ca^{2+} in this capacity. These shifts in voltage dependence are what would be expected if divalent cations can neutralize surface charge. This explains why removal of Ca^{2+} and addition of cadmium have different effects on peak K^+ current.

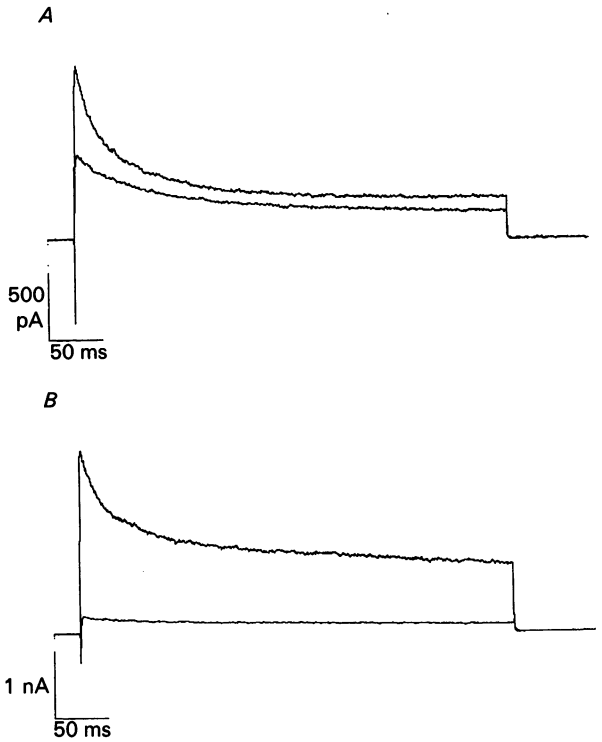

Fig. 15. Block of K^+ current by TEA. Pulses from −100 to +50 mV activated K^+ currents, which were then leak-subtracted. *A*, 1 mM TEA was added to the bathing medium and K^+ current was recorded again to show block, primarily of the rapidly inactivating component. *B*, in a recording from another nerve ending, 5 mM TEA was added to the bathing medium, resulting in stronger block than that observed with 1 mM TEA (*A*). These results are summarized in Table 1.

Pharmacology

K^+ channel blockers have proven very useful in the identification of different K^+ channel types. The K^+ channel blocker tetraethylammonium (TEA) blocked K^+ current in these nerve terminals (Fig. 15). Block of peak current was nearly complete (82%) with 5 mM TEA, and was approximately half (57%) with 1 mM TEA (Table 1). K^+ currents recovered soon after TEA removal. These results are strikingly different from those of Thorn *et al.* (1991) who found that 100 mM TEA had no effect

TABLE 1. TEA effects on whole-cell K^+ current

	Block of fast component (%)	Block of slow component (%)	Block of final current (%)
1 mM TEA ($n = 4$)	67 ± 10	15 ± 10	51 ± 7
5 mM TEA ($n = 4$	90 ± 4	73 ± 9	66 ± 8

K^+ current such as shown in Fig. 15 was recorded before and after the addition of 1 or 5 mM TEA. The transient current was fitted to a sum of two exponentials, as illustrated in Fig. 10, yielding the amplitudes of the two inactivating currents as well as the final non-inactivating K^+ current. Percentage reduction of each component was computed and averaged. The mean percentage reduction is given $\pm$ standard error of the mean.

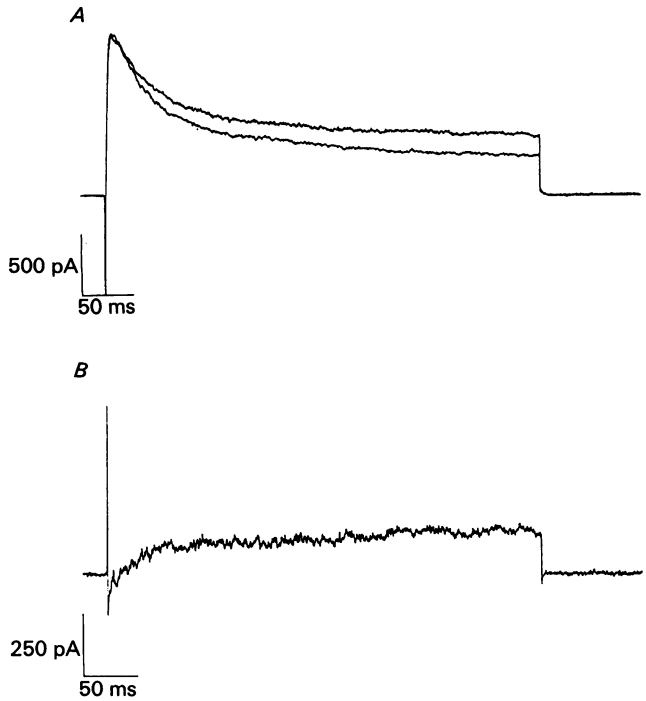

Fig. 16. Block of K^+ current by dendrotoxin. Depolarizing pulses from -100 to $+50$ mV activated K^+ current, which was then leak subtracted. *A* shows control K^+ current and K^+ current from the same nerve terminal following the addition of 50 nM dendrotoxin. The peak current was essentially unaltered by dendrotoxin, while the final current was significantly lower. *B* shows the difference between the two traces shown in *A*. This difference, which is the current blocked by dendrotoxin, was activated in approximately 50 ms and showed no inactivation. This difference current is similar to the average of single-channel traces recorded from a patch containing only the slowly activating K^+ channel (Fig. 7*C*).

on the transient K^+ current in dissociated pituitary nerve terminals. At 5 mM, TEA blocked both components of transient current, as well as the sustained K^+ current (Table 1). With 1 mM TEA some selectivity was evident. As judged from double exponential curve fits such as those shown in Fig. 10, the rapidly inactivating current

was blocked by 67% and the slowly inactivating current was blocked only 15%. Thus the A_f channel has a higher TEA sensitivity than the K^+_{Ca} channel. Current activated by voltage steps from −50 to +50 mV was blocked 64±8% ($n = 4$) by 5 mM TEA, indicating that the non-inactivating K^+ current was also TEA sensitive. We also tested charybdotoxin with concentrations of up to 100 μM and saw no effect on any component of K^+ current in three recordings.

The K^+ channel blocker dendrotoxin also blocked K^+ current in pituitary nerve terminals (Fig. 16). In three of seven recordings, dendrotoxin had no effect. In the other four recordings, the peak current was not significantly reduced (percentage block = 4·6±4·2%; $n = 4$) but the final current was 26±3% lower than controls from the same terminal ($n = 4$). This is consistent with selective block of the D channel. When the current recorded following dendrotoxin application was subtracted from the control current recorded prior to dendrotoxin application, a difference current could be seen (Fig. 16*B*) with a time course very similar to the average of single-channel currents seen in patches containing only the D channel (Fig. 7*C*). The absence of an effect on peak K^+ current indicates that this low concentration of dendrotoxin had little effect on the two transient K^+ channels and was thus quite selective. In some experiments, when an initial application of 20 nM dendrotoxin was followed by application of more dendrotoxin (up to 80 nM), no additional block was observed, indicating that the affinity for the D channel was below 20 nM. In contrast to the action of TEA, the action of dendrotoxin was not reversed after drug removal. No recovery was evident in recordings maintained for up to half an hour.

DISCUSSION

There are at least three distinct K^+ channels in the membranes of rat posterior pituitary nerve endings. These channels could be distinguished on the basis of single-channel conductance, activation kinetics, Ca^{2+} sensitivity, and drug sensitivity. The A_f channel had a conductance of 32 pS, was activated in 1·5 ms or less by test pulses to +60 mV, exhibited voltage-independent inactivation with a time constant of 18 ms at +50 mV, was strongly enhanced by hyperpolarization, and had a relatively low threshold for activation. Furthermore, this channel was more sensitive to TEA than the other transient K^+ channel described here. The K^+_{Ca} channel had a large conductance of 134 pS. It too was activated in 1·5 ms or less by test pulses to +60 mV, but it was inactivated with a time constant of 71 ms, and the rate of inactivation of this channel was voltage dependent. This channel had a higher voltage threshold for activation, and was less sensitive to TEA. The K^+_{Ca} channel was the only one of these three K^+ channels to be sensitive to intracellular Ca^{2+}. The D channel had a conductance of 27 pS, was activated with a time constant of 65 ms, and showed no significant inactivation during test pulses as long as 1 s. This channel had a high voltage threshold for activation, and was blocked by TEA and dendrotoxin. These properties are summarized in Table 2.

The two transient K^+ channels produced whole-cell currents much like other transient currents generally referred to as A currents (Connor & Stevens, 1971; Rogawski, 1985). The macroscopic currents reported here are similar in some

TABLE 2. Summary of channel properties

Channel	Conductance (pS)	Activation at +60 mV (ms)	Inactivation (ms)	Threshold (mV)	TEA, 50% block (mM)	Dendrotoxin 50% block (nM)	Ca^{2+} activation
A_f	32	$\leqslant 1{\cdot}5$	18	< -30	< 1	No	No
K^+_{Ca}	134	$\leqslant 1{\cdot}5$	71	≈ 0	< 5	No	Yes
D	27	65	No	> -30	< 5	< 20	No

respects to those described by Thorn *et al.* (1991). However, K^+ current activation was considerably faster in our study. Another difference was evident in the time constant of slow inactivation, which Thorn *et al.* (1991) found to be voltage insensitive. Furthermore, the mid-point of −87 mV for enhancement by prior hyperpolarization reported here was quite different from the value of −48 mV obtained by Thorn *et al.* (1991). Finally, we found that 1 mM TEA produced a 67% block of the rapidly inactivating component, which is consistent with the sensitivity of hormone release to TEA (Bondy *et al.* 1987; Hobbach *et al.* 1988), while Thorn *et al.* (1991) applied up to 100 mM TEA without observing any inhibition of K^+ current. It is difficult to account for these divergent results, but one likely explanation is that there are differences between K^+ channels when studied in slices or following dissociation. Another possibility is that there are differences between the vasopressin and oxytocin terminals, which could be sampled from unequally depending on whether one is recording from an intact or dissociated preparation.

The conductance of the A_f channel is similar to that of transient K^+ channels in guinea-pig sensory cells (Kasai, Kameyama, Yamaguchi & Fukuda, 1986) and drosophila muscle (Zagotta & Aldrich, 1990). Similar transient K^+ currents have been described in the cell bodies of neurons from many brain regions, including the magnocellular hypothalamic neurons from which these nerve terminals originate (Bourque, 1988; Cobbett *et al.* 1989). The transient outward current described in the cell bodies resembles the A_f channel that we found in the nerve endings. These currents were qualitatively similar in many of the kinetic details, including activation and inactivation rates. The voltage dependence of the activation rate was also similar. The slight decrease in the time constant of inactivation in cell bodies with increasing membrane potential (Cobbett *et al.* 1989) is not inconsistent with the apparent voltage independence described here (Fig. 10). The mid-point of −80 mV for enhancement by hyperpolarization was similar to our value of −87 mV. Finally, TEA reduced the transient K^+ current of cell bodies. These similarities suggest that the A_f channel is expressed in both the cell bodies and nerve terminals of hypothalamic magnocellular neurons.

The K^+_{Ca} channel is activated by intracellular Ca^{2+} and its conductance is similar to the large type Ca^{2+}-activated K^+ channel seen in many other secretory preparations (Marty, 1981; Wong *et al.* 1982; Marty & Neher, 1985). Ca^{2+}-activated K^+ channels have been demonstrated in other nerve endings, including the squid giant synapse (Augustine & Eckert, 1982), mouse (Mallart, 1985) and lizard (Lindgren & Moore, 1989) motor nerve endings, rat brain synaptosomes (Bartschat & Blaustein, 1984), crab peptidergic terminals (Lemos *et al.* 1986) and frog neurohypophysis (Obaid *et al.* 1989; Obaid & Salzberg, 1991). A detailed

characterization of the K^+_{Ca} channel should provide an interesting comparison with other large conductance Ca^{2+}-activated K^+ channels. The channel described here is unusual in that it is insensitive to charybdotoxin. Furthermore, it can be activated at low $[Ca^{2+}]_i$, as indicated by whole-cell recordings made with patch pipettes containing 10 mM EGTA. It has no absolute requirement for Ca^{2+} entry, as cadmium did not reduce the peak K^+ current and channels could be observed in cell-attached patches with pipettes containing 10 mM EGTA. Depolarizing pulses of a few hundred milliseconds produced large increases in $[Ca^{2+}]_i$ (Jackson *et al.* 1991), while under similar conditions the effect of Ca^{2+} entry on K^+ current only developed after nearly 1 s (Fig. 12*B*). This suggests that the increase in activity of the Ca^{2+}-activated K^+ channel lags behind the increase in $[Ca^{2+}]_i$, possibly due to slow Ca^{2+} binding or slow channel activation kinetics. It is difficult to compare the K^+_{Ca} channel with the Ca^{2+}-activated K^+ channel of the cell bodies from which these nerve endings originate, because the two relevant studies in explants (Bourque, 1988) and dissociated cells (Cobbett *et al.* 1989) are not in complete agreement. Thus, at present we cannot say whether the same Ca^{2+}-activated K^+ channel is present in both the nerve endings and cell bodies.

The delayed rectifier channel of hypothalamic neurons (Cobbett *et al.* 1989) may be restricted to nerve cell bodies, since it was not detected in the membranes of the nerve endings. The D channel of our preparation may be related to a delayed rectifier channel, but its activation was much slower than that found by Cobbett *et al.* (1989). Likewise, no evidence was presented for the existence in hypothalamic cell bodies of the D channels described in the present study, suggesting that this channel is restricted to nerve terminals. Both our study in nerve terminals and the study by Cobbett *et al.* (1989) in the cell bodies from which these nerve terminals arise identified three different K^+ channels. Depending on how the hypothalamic Ca^{2+}-activated K^+ channels and K^+_{Ca} channels compare, and whether the studies in terminals and soma sample the same population of cells, hypothalamic peptidergic neurons may possess four or more different K^+ channel types. Some of the K^+ channels may have different cellular locations, where they presumably carry out different physiological functions.

The two transient K^+ channels (including the K^+_{Ca} channel) were activated within 1·5 ms by test pulses comparable in amplitude to an action potential. Action potential width at half-height was approximately 1·8 ms in the absence of high frequency stimulation (Jackson *et al.* 1991). Thus, these two K^+ channels can repolarize action potentials. Given the high current densities in the membrane of neurohypophysial nerve endings, action potential repolarization is probably a major function of these channels. These two channels could thus play an important role in the regulation of peptide secretion. The sensitivity of the two transient K^+ channels to TEA provides pharmacological evidence for such a physiological function, since TEA has been shown to enhance hormone release from the posterior pituitary (Bondy *et al.* 1987; Hobbach *et al.* 1988), presumably by broadening action potentials (Bondy *et al.* 1987; Jackson *et al.* 1991).

Frog Ranvier node has a K^+ channel with properties similar to the D channel (Dubois, 1981). Because of its slow activation kinetics, this channel cannot play a role in action potential repolarization. It may be that this channel is activated during

the long bursts of activity known to occur in the hypothalamic–neurohypophysial system. Opening this channel could raise the threshold for action potential generation. This could then limit secretion towards the end of a long burst. The activation of the K^+ channel could then play a role in the fatigue of stimulus–secretion coupling in the posterior pituitary (Bicknell *et al.* 1984). The K^+_{Ca} channel could also contribute to fatigue of secretion. This fatigue was selective for vasopressin secretion; oxytocin secretion was relatively uniform for long and short stimuli (Bicknell *et al.* 1984). It is thus intriguing that approximately half (3 of 7) of the nerve terminals were insensitive to dendrotoxin, and would then appear to lack the D channel.

Because the A_f and K^+_{Ca} channels were activated rapidly enough to influence action potential duration, it is of particular interest that they both exhibit inactivation. K^+ channel inactivation has recently been proposed as a mechanism underlying action potential broadening and frequency-dependent facilitation in the posterior pituitary (Jackson *et al.* 1991). The preferential block by TEA of the A_f channel described here, together with the preferential enhancement by TEA of release induced by low frequency stimulation (Hobbach *et al.* 1988) fits nicely with this interpretation. Action potential duration has been shown to be a critical determinant of synaptic efficacy in the squid synapse (Augustine, 1990), and also makes an important contribution to synaptic plasticity in *Aplysia* (Hochner *et al.* 1986) and in the club endings on the goldfish Mauthner cell (Lin & Faber, 1988). The two inactivating K^+ channels that we have characterized in neurohypophysial membranes could therefore be important membrane components that may have functions in a wide variety of synaptic systems where there is frequency-dependent coding. Since these two transient K^+ channels have significantly different properties, it is likely that they have different functional roles in the frequency and pattern dependence of secretion.

It is also of interest that the two transient K^+ channels, which are indicated in this study as contributing to action potential repolarization, can be strongly enhanced by hyperpolarization, and virtually eliminated by depolarization. This would suggest that changes in the resting membrane potential would have a profound influence on secretion. A neurotransmitter that altered the nerve ending membrane potential could then have a very strong effect on the amount of transmitter release induced by a presynaptic action potential. Even relatively small neurotransmitter-induced presynaptic depolarizations would make action potentials much broader and more efficacious in secretion, while neurotransmitter-induced presynaptic hyperpolarization would make action potentials very brief and inefficacious in secretion.

This work was initiated while one of us (M. B. J.) was a guest of Dr Arthur Konnerth at the Max Planck Institute for Biophysical Chemistry in Göttingen, and we would like to thank Dr Konnerth for his support. We thank George Augustine and Larry Trussell for helpful comments on this manuscript, and Scarlett Presley for a final proof-reading. This work was supported by NIH grant NS30016.

REFERENCES

AUGUSTINE, G. J. (1990). Regulation of transmitter release at the squid giant synapse by presynaptic delayed rectifier potassium current. *Journal of Physiology* **431**, 343–364.

AUGUSTINE, G. J. & ECKERT, R. (1982). Calcium-dependent potassium current in squid presynaptic nerve terminals. *Biological Bulletin* **163**, 397.

BARTSCHAT, D. K. & BLAUSTEIN, M. P. (1984). Calcium-activated potassium channels in presynaptic nerve terminals. In *Calcium, Neuronal Function and Transmitter Release*, ed. RAHAMIMOFF, R. & KATZ, B., pp. 65–83. Martinus Nijhoff Publishing, Boston.

BENOIT, P. R. & MAMBRINI, J. (1970). Modification of transmitter release by ions which prolong the presynaptic action potential. *Journal of Physiology* **210**, 681–695.

BICKNELL, R. J., BROWN, D., CHAPMAN, C., HANCOCK, P. D. & LENG, G. (1984). Reversible fatigue of stimulus–secretion coupling in the rat neurohypophysis. *Journal of Physiology* **348**, 601–613.

BONDY, C. A., GAINER, H. & RUSSELL, J. T. (1987). Effects of stimulus frequency and potassium channel blockage on the secretion of vasopressin and oxytocin from the neurohypophysis. *Neuroendocrinology* **46**, 258–267.

BONDY, C. A., WHITNALL, M. H., BRADY, L. S. & GAINER, H. (1989). Coexisting peptides in hypothalamic neuroendocrine systems: Some functional implications. *Cellular and Molecular Neurobiology* **9**, 427–446.

BOURQUE, C. W. (1988). Transient calcium-dependent potassium current in magnocellular neurosecretory cells of the rat supraoptic nucleus. *Journal of Physiology* **397**, 331–347.

BOURQUE, C. W. (1990). Intraterminal recordings from the rat neurohypophysis *in vitro*. *Journal of Physiology* **421**, 247–262.

CARL, A. & SANDERS, K. M. (1989). Ca^{2+}-activated channels of canine colonic myocytes. *American Journal of Physiology* **257**, C470–480.

CAZALIS, M., DAYANATHI, G. & NORDMANN, J. (1985). The role of patterned burst and interburst interval on the excitation-coupling mechanism in the isolated neural lobe. *Journal of Physiology* **369**, 45–60.

COBBETT, P., LEGENDRE, P. & MASON, W. T. (1989). Characterization of three types of potassium current in cultured neurones of rat supraoptic nucleus area. *Journal of Physiology* **410**, 443–462.

CONNOR, J. A. & STEVENS, C. F. (1971). Voltage clamp studies of a transient outward membrane current in gastropod neural somata. *Journal of Physiology* **213**, 21–30.

DOUGLAS, W. W. & POISNER, A. M. (1963). Stimulus–secretion coupling in a neurosecretory organ: the role of calcium in the release of vasopressin from the neurohypophysis. *Journal of Physiology* **172**, 1–18.

DREIFUSS, J. J., KALNINS, I., KELLY, J. S. & RUF, J. B. (1971). Action potentials and release of neurohypophysial hormones *in vitro*. *Journal of Physiology* **215**, 805–817.

DUBOIS, J. M. (1981). Evidence for the existence of three types of potassium channels in the frog Ranvier node membrane. *Journal of Physiology* **318**, 297–316.

DUTTON, A. & DYBALL, R. E. J. (1979). Phasic firing enhanced vasopressin release from the rat neurohypophysis. *Journal of Physiology* **290**, 433–440.

EDWARDS, F. A., KONNERTH, A., SAKMANN, B. & TAKAHASHI, T. (1989). A thin slice preparation for patch clamp recordings from neurones of the mammalian central nervous system. *Pflügers Archiv* **414**, 600–612.

GAINER, H. (1978). Input–output relations of neurosecretory cells. In *Comparative Endocrinology*, ed. GAILLARD, P. J. & BOER, H. H., pp. 293–304. Elsevier Biomedical Press, Amsterdam.

GAINER, H., WOLFE, S. A., OBAID, A. L. & SALZBERG, B. M. (1986). Action potentials and frequency-dependent secretion in the mouse neurohypophysis. *Neuroendocrinology* **43**, 557–563.

HAGIWARA, S., KUSANO, K. & SAITO, N. (1961). Membrane changes of *Onchidium* nerve cell in potassium-rich media. *Journal of Physiology* **155**, 470–489.

HAMILL, O. P., MARTY, A., NEHER, E., SAKMANN, B. & SIGWORTH, F. J. (1981). Improved patch-clamp techniques for high-resolution current recording from cells and cell-free membrane patches. *Pflügers Archiv* **391**, 85–100.

HOBBACH, H. P., HURTH, S., JOST, D. & RACKÉ, K. (1988). Effects of tetraethylammonium ions on frequency-dependent vasopressin release from the rat neurohypophysis. *Journal of Physiology* **397**, 539–554.

HOCHNER, B., KLEIN, M., SCHACHER, S. & KANDEL, E. R. (1986). Action-potential duration and the modulation of transmitter release from the sensory neurons of *Aplysia* in presynaptic facilitation and behavioural sensitization. *Proceedings of the National Academy of Sciences of the USA* **83**, 8410–8414.

JACKSON, M. B. (1992*a*). Cable analysis with the whole-cell patch clamp: Theory and experiment. *Biophysical Journal* **61**, 756–766.

JACKSON, M. B. (1992*b*). Passive current flow and morphology in the terminal arborizations of the posterior pituitary. *Journal of Neurophysiology* (in the Press).

JACKSON, M. B., KONNERTH, A. & AUGUSTINE, G. J. (1991). Action potential broadening and frequency-dependent facilitation of calcium signals in pituitary nerve terminals. *Proceedings of the National Academy of Sciences of the USA* **88**, 380–384.

JAN, Y. N., JAN, L. Y. & DENNIS, M. J. (1977). Two mutations of synaptic transmission in *Drosophila*. *Proceedings of the Royal Society* B **198**, 87–108.

KANDEL, E. R. & SCHWARTZ, J. H. (1982). Molecular biology of learning: modulation of transmitter release. *Science* **218**, 433–443.

KASAI, H., KAMEYAMA, M., YAMAGUCHI, K. & FUKUDA, J. (1986). Single transient K^+ channels in mammalian sensory neurons. *Biophysical Journal* **49**, 1243–1247.

LEMOS, J. R., NORDMANN, J. J., COOKE, I. M. & STUENKEL, E. L. (1986). Single channels and ionic currents in peptidergic nerve terminal. *Nature* **319**, 410–412.

LEMOS, J. R. & NOWYCKY, M. C. (1989). Two types of calcium channels coexist in peptide-releasing vertebrate nerve terminals. *Neuron* **2**, 1419–1426.

LIM, N. F., NOWYCKY, M. C. & BOOKMAN, R. J. (1990). Direct measurement of exocytosis and calcium currents in single vertebrate nerve terminals. *Nature* **344**, 449–451.

LIN, J.-W. & FABER, D. S. (1988). Synaptic transmission mediated by single club endings on the goldfish Mauthner cell. II. Plasticity of excitatory postsynaptic potentials. *Journal of Neuroscience* **8**, 1313–1325.

LINDGREN, C. A. & MOORE, J. W. (1989). Identification of ionic currents at presynaptic nerve endings of lizard. *Journal of Physiology* **414**, 201–222.

MALLART, A. (1985). A calcium-activated potassium current in motor nerve terminals of the mouse. *Journal of Physiology* **368**, 577–591.

MARTY, A. (1981). Ca-dependent K channels with large unitary conductance in chromaffin cell membrane. *Nature* **291**, 497–500.

MARTY, A. & NEHER, E. (1983). Tight-seal whole-cell recording. In *Single-Channel Recording*, ed. SAKMANN, B. & NEHER, E., pp. 107–122. Plenum Press, New York.

MARTY, A. & NEHER, E. (1985). Potassium channels in cultured bovine adrenal chromaffin cells. *Journal of Physiology* **367**, 117–141.

MASON, W. T. & DYBALL, R. E. J. (1986). Single ion channel activity in peptidergic nerve terminals of the isolated rat neurohypophysis related to stimulus of neural stalk axons. *Brain Research* **383**, 279–286.

NEHER, E. (1971). Two fast transient current components during voltage clamp of snail neurons. *Journal of General Physiology* **58**, 36–53.

NORDMANN, J. J. (1983). Stimulus–secretion coupling. *Progress in Brain Research* **60**, 281–304.

NORDMANN, J. J. & STUENKEL, E. L. (1986). Electrical properties of axons and neurohypophysial nerve terminals and their relationship to secretion in the rat. *Journal of Physiology* **380**, 521–539.

OBAID, A. L., FLORES, R. & SALZBERG, B. S. (1989). Calcium channels that are required for secretion from intact nerve terminals of vertebrates are sensitive to ω-conotoxin and relatively insensitive to dihydropyridines. *Journal of General Physiology* **93**, 715–729.

OBAID, A. L. & SALZBERG, B. M. (1991). Spike broadening in mammalian and amphibian nerve terminals: Different properties and conductances. *Biophysical Journal* **59**, 595*a*.

OXFORD, G. S. & WAGONER, P. K. (1989). The inactivating K^+ current in GH_3 pituitary cells and its modification by chemical reagents. *Journal of Physiology* **410**, 587–612.

ROGAWSKI, M. A. (1985). The A-current: How ubiquitous a feature of excitable cells is it? *Trends in Neurosciences* **8**, 214–219.

SALZBERG, B. M., OBAID, A. L., SENSEMAN, D. M. & GAINER, H. (1983). Optical recording of action potentials from nerve terminals using potentiometric probes provides evidence for sodium and calcium components. *Nature* **306**, 36–40.

SALZBERG, B. M. & OBAID, A. L. (1988). Optical studies of the secretory event at vertebrate nerve terminals. *Journal of Experimental Biology* **139**, 195–231.

SHAW, F. D., BICKNELL, R. J. & DYBALL, R. E. J. (1984). Facilitation of vasopressin release from the neurohypophysis by application of electrical stimuli in bursts. *Neuroendocrinology* **39**, 371–376.

THORN, P. J., WANG, X. & LEMOS, J. R. (1991). A fast transient K^+ current in neurohypophysial nerve terminals of the rat. *Journal of Physiology* **432**, 283–312.

WONG, B. S., LECAR, H. & ADLER, M. (1982). Single calcium-activated potassium channels in clonal anterior pituitary cells. *Biophysical Journal* **39**, 313–317.

ZAGOTTA, W. N. & ALDRICH, R. W. (1990). Voltage-dependent gating of *Shaker* A-type potassium channels in *Drosophila* muscle. *Journal of General Physiology* **95**, 29–60.